FULL PAPER

Dalton
www.rsc.org/dalton

Controlled and uncontrolled crystallization of calcium oxalate monohydrate in the presence of citric acid

Jian-Ming Ouyang * and Sui-Ping Deng
Institute of Biomineralization and Lithiasis Research, Jinan University, Guangzhou 510632, P. R. China

Received 22nd April 2003, Accepted 4th June 2003
First published as an Advance Article on the web 23rd June 2003

The nucleation and growth of calcium oxalate monohydrate (COM) crystals beneath stearic acid (SA) monolayers in the presence of citric acid (H_3cit) was examined at different surface pressures. The results were compared with those of crystals grown in bulk solution. In bulk solution, the morphology of the precipitated COM crystals transformed from the ($\bar{1}01$) face being most exposed to the (010) face being exposed when the concentration of H_3cit increased from 0.01 to 0.30 mmol L^{-1}. This resulted in a morphological change of the COM crystals from elongated hexagonal to rhombic. At the SA monolayers, the ($\bar{1}01$) faces of the COM crystals were remarkably stabilized independent of either the change in H_3cit concentration from 0.01 to 0.30 mmol L^{-1} or the change in the surface pressure of the SA monolayer from 1 to 20 mN m^{-1}. This result was due to the fact that the ($\bar{1}01$) face of the COM crystals is a Ca^{2+}-rich face, and the carboxylic groups in the headgroups of the SA monolayers and H_3cit are negatively-charged. There is a strong interaction between the ($\bar{1}01$) face of the COM crystals and the negatively-charged carboxylic groups. However, the size of the COM crystals grown at low surface pressures is larger and the crystals more ordered than those grown at high surface pressures. This indicates that the monolayers at low surface pressure have a greater dynamic freedom and compressibility than those at high pressure. This allows the monolayers to reorganize themselves in order to optimize the geometrical and stereochemical fit and then to accommodate the nucleating or growing crystals. H_3cit can inhibit both the nucleation and growth of COM crystals in aqueous solution and at monolayers. Furthermore, H_3cit can reduce the order of COM crystals grown at SA monolayers because H_3cit disturbs the ordered array of the first layer of COM nuclei at the monolayer surface.

1 Introduction

Langmuir monolayers have been used as models for investigating the nucleation and growth of biominerals at organized organic surfaces. The investigated crystals include $CaCO_3$,[1,2] calcium oxalate (CaOxa),[3–7] $CuSO_4 \cdot 5H_2O$,[8,9] $Na_2SO_4 \cdot 7H_2O$,[9] KH_2PO_4,[10] hydroxyapatite,[11] Fe_3O_4, CdS, CdSe, PbS, ZnS, BaS, and NaCl, *etc*.[12] The principal benefit of monolayer model systems is that the composition and physical state of the lipid interface can be controlled. Such systems can serve as models for domains of pure lipid in cellular media.[5]

CaOxa is the most frequent crystalline phase found in human (kidney) stones and occurs in about 70–80%[13,14] of stones found in the inhabitants of industrialized countries. About 40% of the total composition of the calculi is found to be purely calcium oxalate and it also occurs along with calcium phosphates and/or apatites.[15] Deposition of calcium oxalate is also found in the heart and central nervous system *etc*.[16]

However, the mechanism for the formation of the stones is not yet clearly understood and a number of questions about the promoting and inhibiting factors still remain unanswered. The therapeutic efforts are neither clinically nor scientifically satisfactory. The absence of a realistic concept of renal stone generation in an important number of cases is, to a considerable extent, caused by the fact that this process cannot be observed directly *in vivo* and all hypotheses have to be based on results of *in vitro* experiments. The relevance of *in vitro* experiments to urolithiasis depends on the degree of correspondence between the experimental conditions and those prevailing in the stone-forming kidney.[17,18]

In the past decade, an important part of the study of urinary stone formation is to develop an understanding of the interactions between the stone crystals and the components of the organic matrix. Since normal biominerals such as bone and teeth, and abnormal biominerals such as pearl, dental calculus and spur, *etc*. are usually formed within membrane-bound microspaces, and nucleation and growth of the biominerals are regulated by an organic matrix,[19,20] some ordered systems such as Langmuir monolayers[3–7] and vesicles[21] were designed as model systems to mimic the formation of calcium oxalate stones.

On the other hand, some citrates[22,23] and tartrates have been shown to be potent substances that can cure urolithiasis. For example, over the past decades, alkali citrate supplements have been used for the treatment of idiopathic calcium urolithiasis[24] because they increase the solubility of several stone-forming minerals. Potassium sodium citrate is preferred in central Europe while potassium citrate is used in North America.[25]

The possible inhibiting influence of 61 oxyacids,[26] and some amino acids (aspartic, ornithine, tryptophan, hippuric acid, α-ketoglutaric acid, *etc*.)[27,28] on the CaOxa growth process in solution and the type of Ca-oxalate phase formed has been discussed in the literature. We have investigated the effects of various acids and their sodium salts on the crystallization of CaOxa in liposomes[21] and in silica gel systems.[29] The growth and aggregation of calcium oxalate monohydrate (COM) crystals beneath dipalmitoylphosphatidylcholine monolayers in the presence of chondroitin sulfate A, a urinary macromolecule, and glutamic acid was also examined under different surface pressures.[7] The results showed that the crystallization of CaOxa in the controlled systems is very different from that in common aqueous solution.

However, up to now, there has been no report on the crystallization of CaOxa beneath monolayers or at the interface of Langmuir–Blodgett films in the presence of carboxylic acids. If the nucleation, growth, and aggregation of CaOxa crystals can be investigated at the organized monolayers in the presence of a urinary inhibitor such as citric acid, then this model system would be a closer representation of the real mineralization circumstances. With this in mind, the crystallization of CaOxa crystals under stearic acid monolayers in the presence of citric acid has been investigated.

DOI: 10.1039/b304319c

2 Experimental

2.1 Reagents

Stearic acid (SA), citric acid (H_3cit), and other chemicals were purchased from Sigma or Fluka and used without further purification. Milli-Q water with 18.2 MΩ cm resistance was used for subphases and for preparation of all solutions. Stock solutions of 10 mM calcium chloride, 10 mM sodium oxalate and H_3cit were prepared using a TrisHCl buffer (pH 6.0) containing 10.0 mM sodium chloride and were filtered through a 0.22 μm Millipore filter. pH measurements were done by a combination of glass/saturated calomel electrode standardized before and after each experiment with buffer solutions at 25 °C.

2.2 Apparatus

Measurements of surface pressure–area (π–A) isotherms were carried out with a KSV Instruments model 3000 LB system. The surface pressure was measured with a platinum Wihelmy plate connected to a KSV microbalance. Scanning electron microscopy (SEM) was performed using a Philips XL-30 ESEM scanning electron microscope, operating at 10 kV. X-Ray diffraction (XRD) results were recorded on a D/max-γA X-ray diffractometer (Japan), using Ni-filtered Cu-K_α radiation (λ = 0.154 nm), the scanning rate was 2° min^{-1}. The divergence and scattering slit was at 1° for $5 < 2\theta < 60°$. FT-IR spectra were recorded with a Bruker IFS25 FT-IR spectrometer (Bruker Spectrospin, Wissembourg, France) between 4000 and 400 cm^{-1} with a resolution of 4 cm^{-1}.

2.3 Methods

A solution of SA in chloroform (concentration: 1.0 mmol L^{-1}) was spread onto a subphase containing 0.30 mmol L^{-1} CaOxa using a microsyringe. After the chloroform had evaporated (*ca.* 30 min), the monolayer was compressed to the desired surface pressure at a rate of *ca.* 0.03 nm^2 molecule^{-1} min^{-1}. The estimated error in the isotherm area measurements is ±0.01 nm^2 molecule^{-1}. The CaOxa subphase was prepared according to reference 3.

The transfer of CaOxa crystals grown beneath the monolayers to solid supports for analysis by SEM and XRD was accomplished by carefully draining the subphase from the trough to lower the monolayer onto a substrate that had been placed in the subphase before the monolayer was applied. Substrates were positioned at an angle of approximately 35° with respect to the bottom of the trough to allow for better drainage.

Additional crystal growth experiments were performed in crystallization dishes (diameter = 6.2 cm, depth = 3.0 cm).[4] The amount of SA spread at the interface was adjusted to achieve approximately the same surface pressure as in the trough experiments. The crystallization dishes were sealed with glass covers to slow down evaporation. Since the area per molecule in these studies is not as well controlled as in the trough studies, this method was only used for preliminary crystal growth studies. The final SEM images were obtained from crystals grown in the trough.

All work was carried out in a dust-free box at a temperature of 25 °C. The experiments were repeated at least twice.

3 Results

3.1 Uncontrolled crystallization of COM crystals in the presence of citric acid

Fig. 1 shows the SEM images of calcium oxalate crystals grown in aqueous solution in the presence of 0.10 and 0.30 mmol L^{-1} H_3cit, respectively. Spectroscopic examination by X-ray diffraction (XRD) and FT-IR spectroscopy confirmed the exclusive formation of calcium oxalate monohydrate (COM). In the

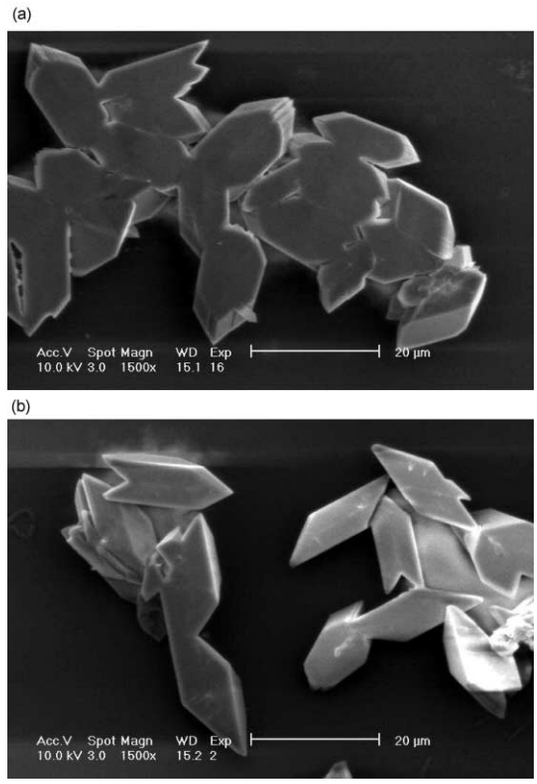

Fig. 1 SEM images of COM crystals grown in aqueous solution in the presence of (a) 0.10 and (b) 0.30 mmol L^{-1} H_3cit (crystallization time 1 d, c(CaOxa) = 0.30 mM, the bar = 20 μm).

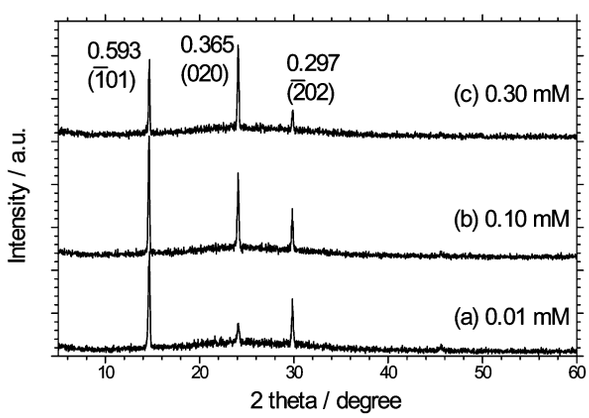

Fig. 2 XRD patterns of the COM crystals grown in aqueous solution in the presence of various concentrations of H_3cit.

XRD patterns (Fig. 2), the corresponding main diffraction peaks are located at 0.593, 0.365, and 0.297 nm, which can be assigned to the (1̄01), (020), and (2̄02) planes of the COM crystals, respectively.[30,31] In the FT-IR spectra (Fig. 3), the peaks at 1618 and 1318 cm^{-1} are the main antisymmetric carbonyl stretching bands specific to the oxalate family and the metal–carboxylate stretch, respectively.[13,15,31] In the fingerprint region, three characteristic absorptions are located at 948, 881 and 665 cm^{-1}. All these peaks are in good agreement with the archived data for COM crystals.[13,15]

The morphology of COM was remarkably affected by the concentration of H_3cit. With the increase of the concentration of H_3cit from 0.01 to 0.30 mmol L^{-1}, the content of the COM crystals with the (1̄01) face exposed decreased from 80% to 24%, and that with the (010) face exposed increased from 20% to 76%. This results not only in the (1̄01) diffraction peak becoming gradually weaker (Fig. 2), but also in a morphological change in the COM crystals from elongated hexagonal (Fig. 1a) to rhombic (Fig. 1b). Fig. 4 shows the schematic representation of the morphological change in the COM crystals.

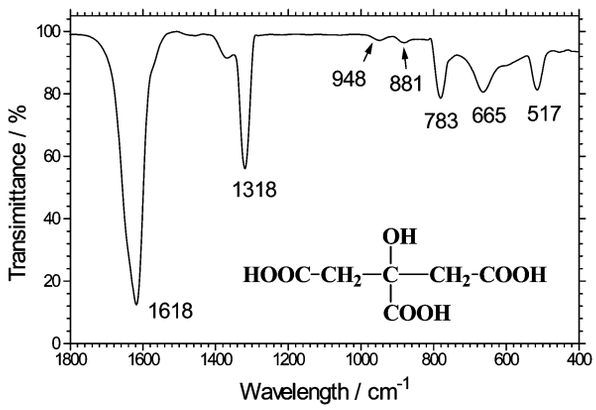

Fig. 3 FT-IR spectrum of COM crystals grown in aqueous solution in the presence of 0.10 mmol L^{-1} H_3cit. The insert shows the molecular structure of citric acid.

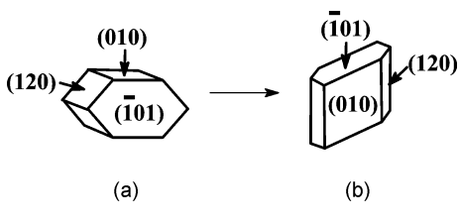

Fig. 4 Schematic representation showing the morphological change in the COM crystals.

3.2 Controlled crystallization of COM crystals at SA monolayers in the presence of H_3cit

Fig. 5 shows the SEM images of COM crystals grown at SA monolayers in the presence of different concentrations of H_3cit. From Fig. 5, four results can be obtained. First, nearly all of the COM crystals were elongated hexagonal crystals with the ($\bar{1}$01) face parallel to the plane of the monolayer. This was apparently different from the results observed in the bulk solution. In the latter case, the COM crystals were composed of both the elongated hexagonal and the rhombic crystals (Fig. 1). Second, the size of the COM crystals was remarkably decreased as the concentration of H_3cit increased. At the SA monolayer without H_3cit, the size of the COM crystals was about 8 × 25 μm in width and length (Fig. 5a). It decreased to about 8 × 15 μm (Fig. 5b) and 5 × 11 μm (Fig. 5c) in the presence of 0.1 and 0.3 mmol L^{-1} H_3cit, respectively. That is, H_3cit can inhibit the growth of COM crystals. Third, the number of COM crystals decreased as the H_3cit concentration increased. This indicates that H_3cit can inhibit the nucleation of COM crystals. Fourth, compared with the orderly growth at monolayers without H_3cit, the COM crystals grew randomly in the presence of H_3cit.

3.3 Effect of surface pressure of SA monolayer on the growth of COM crystals

The effect of H_3cit on the crystallization of COM beneath SA monolayers was investigated at different surface pressures. Fig. 6 shows the SEM images of COM crystals grown in the presence of 0.10 mmol L^{-1} H_3cit at 1 and 20 mN m^{-1}, respectively. Nearly all of the COM crystals grown at 1 and 20 mN m^{-1} show similar morphology as elongated hexagonal crystals. This means that the ($\bar{1}$01) face of the COM crystals preferentially grows parallel to the plane of the SA monolayer. However, the size of the COM crystals (10 × 24 μm, Fig. 6a) grown at low surface pressures of 1 mN m^{-1} is larger than that (9 × 16 μm, Fig. 6b) of those grown at the higher surface pressure of 20 mN m^{-1}. The ordering of the COM crystals at 1 mN m^{-1} is also better than for those grown at 20 mN m^{-1}.

The growth of COM crystals at SA monolayers in the presence of 0.01, 0.03, 0.2, and 0.3 mmol L^{-1} H_3cit showed similar crystallization rules, respectively.

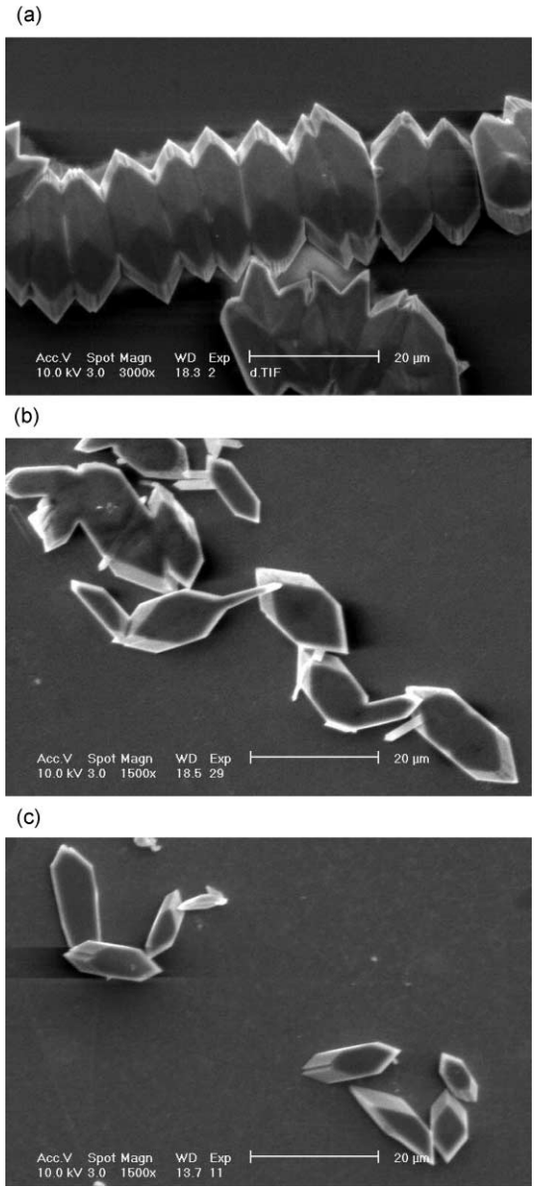

Fig. 5 SEM images of COM crystals grown at SA monolayers at a surface pressure of 20 mN m^{-1} in the absence (a) and in the presence of (b) 0.10 and (c) 0.30 mM H_3cit, respectively (crystallization time 1 d, *c*(CaOxa) = 0.30 mM, the bar = 20 μm).

4 Discussion

4.1 Inhibition of the ($\bar{1}$01) face and induction of the (010) face of COM crystals by H_3cit

As shown in Fig. 1, when the concentration of H_3cit in aqueous solution increased, the content of the COM crystals with the ($\bar{1}$01) face exposed decreased gradually and that with the (010) face exposed increased. At a concentration of 0.01 mmol L^{-1} H_3cit, about 80% of the COM crystals grew with the ($\bar{1}$01) face being most exposed. However, the COM crystals with the (010) face exposed were dominant at a concentration of 0.30 mmol L^{-1} H_3cit (Fig. 1b). This leads to a morphological change of the COM crystals from the elongated hexagonal (Fig. 4a) to the rhombic (Fig. 4b). This is because the ($\bar{1}$01) crystal face of COM is characterized by oxalate ions emerging oblique to the faces with a dense pattern of complexed calcium ions exposed (Fig. 7a). That is, ($\bar{1}$01) is a calcium-ion rich face and there is a positively-charged surface for the ($\bar{1}$01) crystal face of COM crystals.[32,33] On the other hand, the carboxylic groups of H_3cit are negatively-charged, so H_3cit can interact strongly with the densely packed Ca^{2+} ions within the ($\bar{1}$01) face by electrostatic attraction and then block this face against further growth,

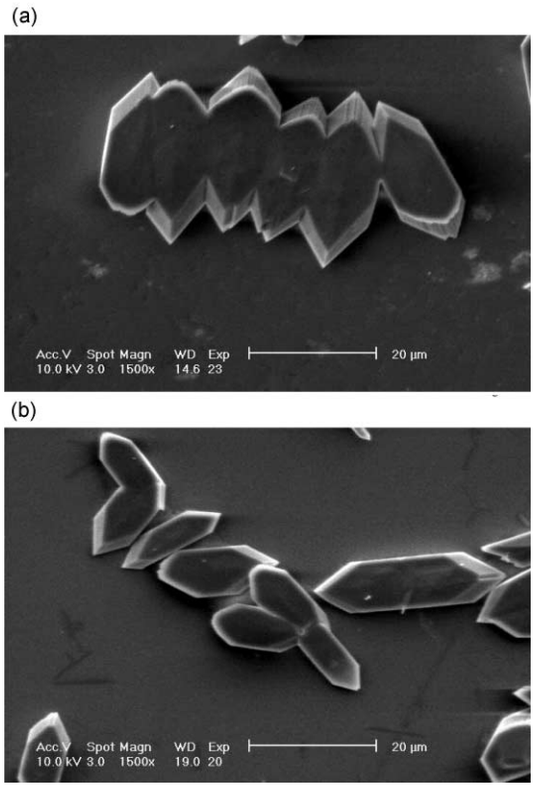

Fig. 6 SEM images of COM crystals grown at SA monolayers at a surface pressure of (a) 1 and (b) 20 mN m^{-1} in the presence of 0.10 mM H_3cit (crystallization time 1 d, *c*(CaOxa) = 0.30 mM, the bar = 20 μm).

whilst stabilizing the face at the same time. In contrast, the (010) face is nearly neutral and contains an alternative arrangement of Ca^{2+} ions and Oxa^{2-} anions (Fig. 7b). The Oxa^{2-} anions lie on the surface with an orientation perpendicular to the (010) face. In this situation, it could be less favorable for the functional groups to interact with this face, leading to a relatively faster growth rate than that of the ($\bar{1}$01) face.

Cody *et al.*[26] once concluded that only linear molecules with carboxyl group spacings of approximately three C–C bond lengths (propane spacing) are shown to inhibit COM formation. That is, a 'fit' relationship between the COM crystal lattice and the structurally-specific molecules is responsible for the inhibition of pre-critical nuclei of COM and for a part of the inhibitor capacity of urine components such as H_3cit. Our results[21] showed that the group $^{-}$OOC–C(OH)–COO^{-} is the functional group for this inhibition. Computer modeling also confirms the structural match between the distance of the carboxylic groups of H_3cit molecules and the distance of the Ca^{2+} ions within the ($\bar{1}$01) plane of COM crystals.[34] The binding affinity of H_3cit is due to its ability to adopt conformations in which three carboxylic groups can interact with the surface of CaOxa.[27]

4.2 Preferential selection of the ($\bar{1}$01) face of COM crystals by SA monolayers

At the SA monolayer all of the COM crystals grow with the ($\bar{1}$01) face exposed (Figs. 5 and 6). There are fewer COM crystals with the (010) face being most exposed. This was found to be independent of the surface pressure of the SA monolayer at 1 as well as at 20 mN m^{-1}. This shows that the SA monolayer can markedly stabilize the ($\bar{1}$01) face of COM crystals.

In general, the monolayer has the tendency to form an arrangement that matches the incipient crystal face. The monolayer does not need to be preorganized, but the amphiphiles must be able to achieve a packing necessary to sufficiently concentrate charge and contribute to surface stabilization through selective adsorption. When COM grows under SA

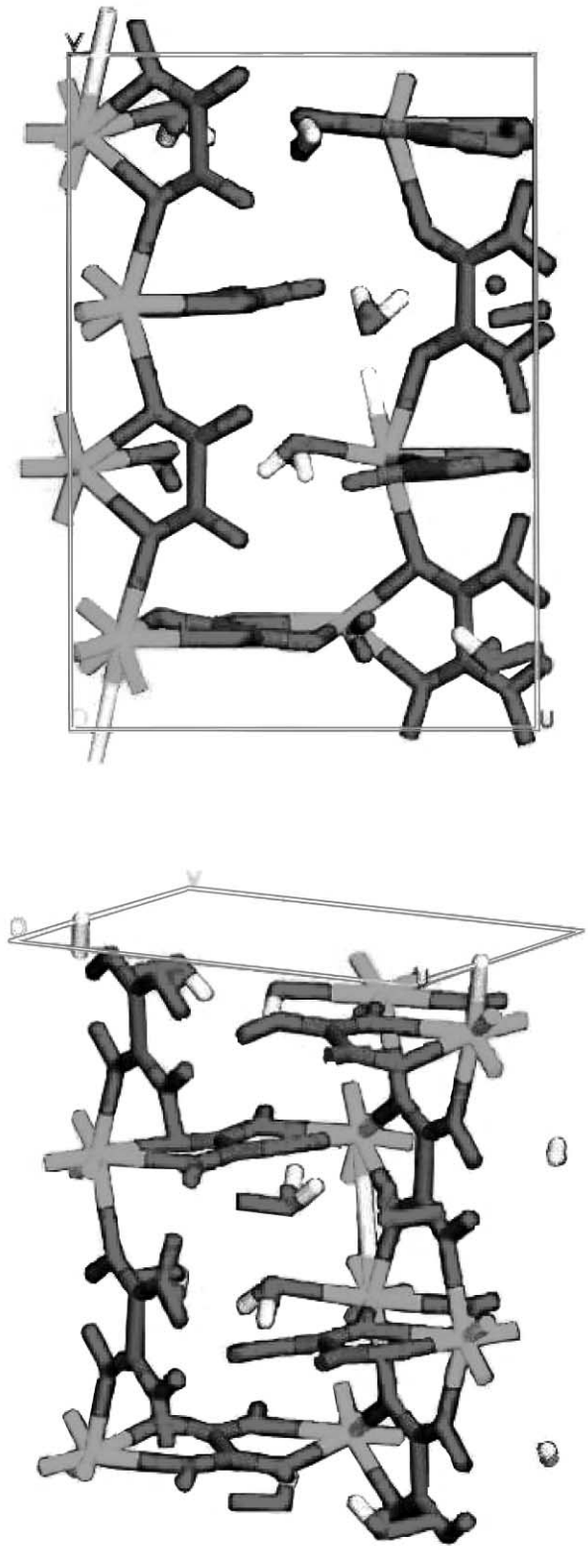

Fig. 7 The surface cleaved plots of COM crystals obtained using Cerius[2] software. (a) Cleaved ($\bar{1}$01) face viewed along the [$\bar{1}$01] direction; (b) cleaved surface along the (010) direction.

monolayers, this monolayer can act as a template for COM growth and leads to a high selectivity for a specific crystal orientation.[3] Since the headgroups of the SA monolayers are the negatively charged carboxylic groups, the two-dimensional crystalline structure of SA monolayers results in ordered and negatively charged "recognized sites". The sites will bind the positive-charged Ca^{2+} ions to the carboxylic headgroups of SA monolayers and thus stimulate nucleation of the COM crystallite with the positively-charged ($\bar{1}$01) face being most exposed at

the monolayer surface due to the decrease of nucleation active energy of the COM crystals. Such a mechanism was proposed previously by Whipps and Khan[5] for the crystallization of CaOxa at phospholipid DPPC monolayers and by Heywood and Mann[2] for the crystallization of $CaCO_3$ at SA monolayers.

It is interesting to compare the critical difference between the carboxylic functional groups of an individual citric acid molecule binding Ca^{2+} ions and that of the combination of carboxylic acids of several stearic acid molecules binding to the growing calcium oxalate monohydrate crystals. The former shows inhibition while the latter shows promotion of the nucleation and growth of COM crystals. This is because H_3cit is a strong chelating agent. The stability constant (K_s) of H_3cit upon forming a 1 : 1 complex with Ca^{2+} ions was $10^{4.68}$.[35] Furthermore, the distance of the COO^- groups of H_3cit can match well the distance of the Ca^{2+} ions within the ($\bar{1}$01) face of COM,[26,34] and then strengthen the inhibition ability of H_3cit. This enables H_3cit able to inhibit strongly the nucleation and growth of COM crystals. However, when many SA molecules form ordered monolayers at the air/water interface, the negatively-charged COO^- headgroups of the monolayers can accumulate the positive Ca^{2+} ions in the bulk solution. The increase in the concentration of Ca^{2+} ions at the monolayer/water interface then promotes the nucleation and growth of the COM crystals as discussed above. Especially at low surface pressures, the SA monolayers with greater dynamic freedom and compressibility can match the ($\bar{1}$01) face of COM well (this will be discussed in detail in Section 4.3), so it preferentially promotes the formation of COM crystals with the ($\bar{1}$01) face exposed.

Animal models[36] have demonstrated that the attachment process of CaOxa crystals to cell membranes appears to be mediated by specific molecular interactions between molecular structures on the surfaces of stone crystals and molecular arrays on the surfaces of cell membranes. The calcium-rich ($\bar{1}$01) crystal face has been implicated in studies of adhesion of COM to membranes in lipid-enriched cell culture studies.

4.3 SA monolayers at low surface pressure catalyze the heterogeneous nucleation and growth of COM crystals

It can be seen from Fig. 6 that at low applied surface pressures the size of the COM crystals is larger than those grown at high surface pressure. The ordering of the COM crystals at 1 mN m^{-1} is also better than for those grown at 20 mN m^{-1}. This result can be due to the following two factors. First, as a negatively-charged surfactant, SA can enrich Ca^{2+} ions at the monolayer/water interfaces, resulting in an increase of the concentration of Ca^{2+} ions at the interface. According to the nucleation and growth theory,[37,38] for heterogeneous nucleation the free energy (ΔG) of formation of a nucleus depends on the level of solution supersaturation (S), the net interfacial free energy for nucleation (σ_{net}), and the surface area of the nuclei (A),

$$\Delta G = -RT\ln S + \sigma_{net}A \qquad (1)$$

where R is the ideal gas constant, T is the absolute temperature, and σ_{net} is composed of the contributions from the interfacial free energy of the crystal particle (σ_c), the substrate (σ_s), and the liquid phase (σ_l). The increase of the supersaturation (S) of CaOxa at the SA monolayer/water interface leads to a decrease in the free energy of heterogeneous nucleation (ΔG), therefore the COM crystals preferentially nucleate at the monolayer/water interface. Once the nuclei are formed, they block the formation of new nuclei under the monolayers. This leads to the growth of larger COM crystals beneath the monolayers. Second, the monolayers at low pressures have a greater dynamic freedom and compressibility.[3,39,40] The monolayer interfaces at low pressure have the ability to optimize the geometrical and stereochemical fit and then to rearrange to accommodate the nucleating or growing crystal. That is, the monolayers of SA at low surface pressure can catalyze heterogeneous precipitation of COM from metastable solutions.

As reported by Deganello *et al.*[41] and Backov *et al.*,[3] the calculated calcium densities for the ($\bar{1}$01) and (010) faces of COM crystals are 0.04 and 0.03 ions $Å^{-2}$, respectively. That is, each Ca^{2+} ion in the ($\bar{1}$01) and (010) faces of COM occupies an area of about 0.25 and 0.33 nm^2, respectively. As shown in Fig. 8, the area per SA molecule in SA monolayers on the subphase containing 0.30 mM CaOxa at 1 and 20 mN m^{-1} is about 0.24 and 0.195 nm^2, respectively. These area values are in good agreement with the archived data.[42] It can be seen that the area per carboxylic group of the SA headgroups at 1 mN m^{-1} (0.24 nm^2) can match the area per Ca^{2+} ion within the ($\bar{1}$01) face of the COM crystals (0.25 nm^2) with a mismatch of about 2.5%.

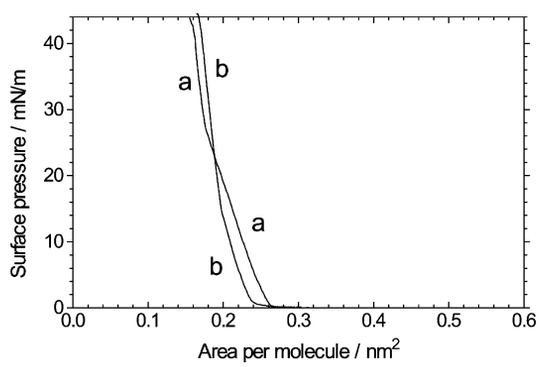

Fig. 8 Surface pressure–area isotherms of SA monolayers on a pure water subphase (a) and a subphase containing 0.30 mM CaOxa (b).

4.4 H_3cit inhibits the nucleation and growth of COM crystals

Figs. 1 and 5 show that the size and number of the COM crystals increased when the concentration of H_3cit was lowered. This is independent of whether the COM crystals were grown beneath the SA monolayers or not. This indicated that H_3cit could inhibit both the nucleation and growth of the COM crystals.

As a tricarboxylic acid, H_3cit has three COOH groups and one hydroxy group (*cf.* the molecular structure of H_3cit in the insert in Fig. 3), so H_3cit is a strong chelating agent towards Ca^{2+} ions. The concentration of free Ca^{2+} ions in the solutions or subphases will be decreased after addition of H_3cit. This makes the size of the COM crystals small. In addition, H_3cit can block the active sites for the growth of COM crystals at the monolayer. It further strengthens the ability of H_3cit to inhibit COM growth and to decrease the formation of COM nuclei.

The formation of kidney stones involves nucleation, growth, and aggregation of stone forming crystals and their retention in the kidneys. If any of the process can be inhibited stone formation can be prevented. H_3cit can inhibit both the nucleation and the growth of CaOxa crystals, so H_3cit can act as a good inhibitor for urolithiasis.

4.5 H_3cit decreases the ordering of COM crystals grown at SA monolayers

From Fig. 5 we can see that the ordering of the COM crystals grown on a pure water subphase is better than those grown on subphases containing H_3cit. In the absence of H_3cit, the SA monolayer arranges itself with high order with its complexing headgroups (COOH group) in contact with the aqueous phase. The ordered array of SA headgroups in the monolayers makes the first layer of Ca^{2+} ions adsorb in an orderly fashion on the monolayers. Then one layer of Oxa^{2-} anions also react in an orderly fashion with the absorbed Ca^{2+} ions. This leads to the formation of COM crystals with good order. Especially when the surface pressure of the SA monolayer is smaller, the

headgroups of the SA monolayer can match the ($\bar{1}$01) face of COM better than at high pressure as discussed above. So the ordering of the COM crystals grown at lower surface pressure is much better than that grown at high pressure.

However, when H_3cit was added to the subphases, the COOH groups of H_3cit become randomly dispersed in the subphases. Both the random COOH groups of H_3cit and the ordered COOH groups of the SA monolayers can react with the Ca^{2+} ions at the monolayer/water interfaces and there is competition between the two types of reaction. Since the ability of H_3cit to coordinate with Ca^{2+} ions is stronger than that of SA with Ca^{2+} ions, the random H_3cit molecules in the subphase have the ability to chelate the Ca^{2+} ions bound by the SA monolayers. This disturbs the ordered array of the first layer of COM nuclei at the monolayer, and results in a lowering of the order of the COM crystals.

5 Conclusions

The investigation on the mechanisms of nucleation and growth of crystals at organic–inorganic interfaces is crucial for understanding biological and physiological calcification processes such as the formation of urinary stones. Therefore the mineralization of calcium oxalate monohydrate (COM) was investigated at stearic acid monolayers in the presence of the urinary inhibitor citric acid at different surface pressures. At SA monolayers, the ($\bar{1}$01) faces of COM crystals were remarkably stabilized independent of either the change of H_3cit concentration from 0.01 to 0.30 mmol L^{-1} or the change of the surface pressure of the SA monolayers from 1 to 20 mN m^{-1}. This result was due to the strong interaction of the Ca^{2+}-rich ($\bar{1}$01) face of the COM crystals with the negatively charged carboxylate headgroups of the SA monolayers.

At a low surface pressure of 1 mN m^{-1}, there is an optimized geometrical and stereochemical match between the SA monolayer and the nucleating or growing COM crystals. The mismatch is about 2.5% between the area per SA molecule in monolayers at 1 mN m^{-1} (0.24 nm^2) and the area per Ca^{2+} ion in the ($\bar{1}$01) face of the COM crystal (0.25 nm^2). This leads to the formation of COM crystals with a large size and good ordering at the SA monolayer at 1 mN m^{-1}.

Previous evidence suggests that the formation of urinary stones includes nucleation, growth, and aggregation of CaOxa crystals in urine as well as subsequent trapping of the crystals within the kidney. H_3cit can effectively inhibit crystal nucleation and growth of COM. It is possible that the existence of H_3cit in urine could provide an alternative tool for markedly restraining the formation of urinary stones.

Acknowledgements

This research work was granted by the Key project of Natural Science Foundation of China (20031010), the Key Project of Guangdong Province (C31401), and the Key project of Natural Science Foundation of Guangdong Province (013202). We are grateful to Dr S.-H. Yu of MPI of Colloids and Interfaces of Potsdam of Germany for providing the crystal face figures.

References

1 S. Mann, B. R. Heywood and S. Rajam, *Nature (London)*, 1988, **334**, 692–695.
2 B. R. Heywood and S. Mann, *Chem. Mater.*, 1994, **6**, 311–318.
3 R. Backov, C. M. Lee, S. R. Khan, C. Mingotaud, G. E. Fanucci and D. R. Talham, *Langmuir*, 2000, **16**, 6013–6019.
4 S. R. Letellier, M. Lochhead and V. Vogel, *Biochim. Biophys. Acta*, 1998, **1380**, 31–45.
5 S. Whipps and S. R. Khan, *J. Cryst. Growth*, 1998, **192**, 243–249.
6 R. Backov, S. R. Khan, C. Mingotaud, K. Byer, C. M. Lee and D. R. Talham, *J. Am. Soc. Nephrol.*, 1999, **10**, S359–S363.
7 J.-P. Zhong, J.-M. Ouyang and S.-P. Deng, *Wuji Huaxue Xuebao*, 2002, **18**, 1253–1257.
8 R. Tang, C. Jiang and Z. Tai, *J. Chem. Soc., Dalton. Trans.*, 1997, 4037–4041.
9 R. Tang, Z. Tai and Y. Chao, *J. Chem. Soc., Dalton Trans.*, 1996, 4439–4441.
10 C. L. Ma, H. B. Lu and R. Z. Wang, *J. Cryst. Growth*, 1997, **173**, 141–149.
11 B. Li, Y. Liu and R. Xu, *Langmuir*, 1999, **15**, 4837–4841.
12 J.-M. Ouyang, *Principle and Applications of Langmuir–Blodgett*, Jinan University Press, Guangzou. 1999, ch. 5.
13 M.-E. Laurence, P. Levillain, B. Lacour and M. Daudon, *Clin. Chim. Acta*, 2000, **298**, 1–11.
14 F. Grases, A. Costa-Bauza, M. Ramis, V. Montesinos and A. Conte, *Clin. Chim. Acta*, 2002, **322**, 29–36.
15 E. K. Girija, S. C. Latha, S. N. Kalkura and C. Subramanian, *Mater. Chem. Phys.*, 1998, **52**, 253–257.
16 M. Deepa, K. R. Babu and V. K. Vaidyan, *J. Mater. Sci. Lett*, 1995, **14**, 1321–1322.
17 J.-M. Ouyang, X.-Q. Yao, Z.-X. Su and F.-Z. Cui, *Sci. China, Ser. B*, 2003, **33**, 14–19.
18 J.-M. Ouyang, X.-Q. Yao, J.-P. Zhong, Y.-S. Xie, Y. Bai, L. Kuan and W.-X. Tang, *Gaodeng Xuexiao Huaxue Xuebao*, 2002, **23**, 2237–2239.
19 P. Calvert and S. Mann, *Nature (London)*, 1997, **386**, 127–130.
20 J.-M. Ouyang, *Chem. Bull.*, 2002, **65**, 326–332.
21 J.-M. Ouyang, L. Duan, J.-H He and B. Tieke, *Chem. Lett.*, 2003, 268–269.
22 H. A. Fuselier and D. M. Ward, *Urology*, 1995, **45**, 942–946.
23 K. Sakhaee, M. Nicar, K. Hill and C. Y. C. Pak, *Kidney Int.*, 1983, **24**, 348–352.
24 P. O. Schwille, U. Herrmann, C. Wolf, I. Berger and R. Meister, *Urol. Res.*, 1992, **20**, 145–155.
25 G. M. Preminger, K. Sakhaee and C. Y. C. Pak, *J. Urol. (Baltimore)*, 1988, **139**, 240–242.
26 A. M. Cody and R. D. Cody, *J. Cryst. Growth*, 1994, **135**, 235–245.
27 D. E. Fleming, W. Bronswijk and R. L. Ryall, *Clin. Sci.*, 2001, **101**, 159–168.
28 F. Grases and J. G. March, *J. Cryst. Growth*, 1988, **87**, 299–304.
29 J.-M. Ouyang, Y. Tan and Y.-H. Shen, *Wuli Huaxue Xuebao*, 2003, **19**, 368–371.
30 *Powder Diffraction File Alphabetic Index, Inorganic Phases/ Organic Phases*, ed. M. King, W. F. McClure, L. C. Andrews and M. A. Holomery, International Center For Diffraction Data, Pennsylvania, USA, 1992, pp. 19081–2389.
31 J.-M. Ouyang, *Guangpuxue Yu Guangpu Fenxi*, 2003, **23**, 391–395.
32 L. Tunik and N. Garti, *J. Cryst. Growth*, 1996, **167**, 748–755.
33 S. R. Khan, P. O. Whalen and P. A. Glenton, *J. Cryst. Growth*, 1993, **134**, 211–218.
34 K. E. Gilbert, PCMODEL, Molecular Modeling Software, Version 4, Serena Software, Bloomington, IN, 1990.
35 *Lange's Handbook of Chemistry*, ed. J. A. Dean, McGraw-Hill, New York, 13th edn., 1985, pp. 5–46.
36 N. Mandel, *J. Am. Soc. Nephrol.*, 1994, **5**, S37–S45.
37 A. A. Campbell, *Curr. Opin. Colloid Interface Sci.*, 1999, **4**, 40–45.
38 M. J. Hounslow, A. S. Bramley and W. R. Paterson, *J. Colloid Interface Sci.*, 1998, **203**, 383–391.
39 S. J. Cooper, R. B. Sessions and S. D. Lubetkin, *J. Am. Chem. Soc.*, 1998, **120**, 2090–2098.
40 S. J. Cooper, R. B. Sessions and S. D. Lubetkin, *Langmuir*, 1997, **13**, 7165–7172.
41 S. Deganello and O. E. Piro, *Neues Jahrb. Mineral., Monatsh.*, 1981(2), 81–88.
42 A.-F. Mingotaud, C. Mingotaud and L. K. Patterson, *Handbook of Monolayers*, Academic Press Inc., San Diego, CA, 1993, p. 16.